British Journal of Pharmacology

British Journal of Pharmacology (2018) **175** 53–66 53

RESEARCH PAPER

FL-926-16, a novel bioavailable carnosinase-resistant carnosine derivative, prevents onset and stops progression of diabetic nephropathy in *db*/*db* mice

Correspondence Giuseppe Pugliese, Department of Clinical and Molecular Medicine, Via di Grottarossa, 1035 – 00189 Rome, Italy. E-mail: giuseppe.pugliese@uniroma1.it

Received 8 May 2017; **Revised** 6 October 2017; **Accepted** 9 October 2017

Carla Iacobini[1,*], Stefano Menini[1,*], Claudia Blasetti Fantauzzi[1], Carlo M Pesce[2], Andrea Giaccari[3], Enrica Salomone[3], Annunziata Lapolla[4], Marica Orioli[5], Giancarlo Aldini[5] and Giuseppe Pugliese[1]

[1]*Department of Clinical Molecular Medicine, 'La Sapienza' University, Rome, Italy,* [2]*DINOGMI, University of Genoa, Genoa, Italy,* [3]*Endo-Metabolic Diseases Unit, Catholic University, Rome, Italy,* [4]*Department of Medicine, University of Padua, Padua, Italy, and* [5]*Department of Pharmaceutical Sciences, University of Milan, Milan, Italy*

*Carla Iacobini and Stefano Menini contributed equally to this work.

BACKGROUND AND PURPOSE

The advanced glycation end products (AGEs) participate in the pathogenesis of diabetic nephropathy (DN) by promoting renal inflammation and injury. L-carnosine acts as a quencher of the AGE precursors reactive carbonyl species (RCS), but is rapidly inactivated by carnosinase. In this study, we evaluated the effect of FL-926-16, a carnosinase-resistant and bioavailable carnosine derivative, on the onset and progression of DN in *db*/*db* mice.

EXPERIMENTAL APPROACH

Adult male *db*/*db* mice and coeval *db*/*m* controls were left untreated or treated with FL-926-16 (30 mg·kg^{-1} body weight) from weeks 6 to 20 (prevention protocol) or from weeks 20 to 34 (regression protocol).

KEY RESULTS

In the prevention protocol, FL-926-16 significantly attenuated increases in creatinine (−80%), albuminuria (−77%), proteinuria (−75%), mean glomerular area (−34%), fractional (−40%) and mean (−42%) mesangial area in *db*/*db* mice. This protective effect was associated with a reduction in glomerular matrix protein expression and cell apoptosis, circulating and tissue oxidative and carbonyl stress, and renal inflammatory markers, including the NLRP3 inflammasome. In the regression protocol, the progression of DN was completely blocked, although not reversed, by FL-926-16. In cultured mesangial cells, FL-926-16 prevented NLRP3 expression induced by RCS but not by the AGE N$^{\varepsilon}$-carboxymethyllysine.

CONCLUSION AND IMPLICATIONS

FL-926-16 is effective at preventing the onset of DN and halting its progression in *db*/*db* mice by quenching RCS, thereby reducing the accumulation of their protein adducts and the consequent inflammatory response. In a future perspective, this novel compound may represent a promising AGE-reducing approach for DN therapy.

Abbreviations

A/C, albumin/creatinine ratio; AGER, advanced glycosylation end-product-specific receptor; AGEs, advanced glycation end products; CML, N$^{\varepsilon}$-carboxymethyllysine; CNDP, carnosine dipeptidase; Ctrl, control; Diab, diabetic; fMA, fractional mesangial area; HNE, 4-hydroxynonenal; IHC, immunohistochemistry; MCP-1, monocyte chemoattractant protein-1; mGA, mean glomerular area; mMA, mean mesangial area; NLRP3, NOD-like receptor family, pyrin domain containing 3; Nox4, renal isoform of NAD(P)H oxidase; P/C, protein/creatinine ratio; PAS, periodic acid Schiff; PCOs, total carbonylated proteins; RCS, reactive carbonyl species

DOI:10.1111/bph.14070

Introduction

Diabetic nephropathy is one of the most common complications of diabetes. As its prevalence has been increasing steeply along with an epidemic in type 2 diabetes (Tuttle *et al.,* 2014), diabetic nephropathy has become the leading cause of end-stage renal disease in western countries, where it accounts for approximately 50% of cases (Harjutsalo and Groop, 2014). The Diabetes Control and Complications Trial and the UK Prospective Diabetes Study have definitively shown that strict glycaemic control is effective at reducing but not eliminating the risk of microalbuminuria and overt diabetic nephropathy (Molitch *et al.,* 2004). In addition, in patients with type 2 diabetes, other coexisting risk factors, such as obesity, dyslipidaemia and hypertension, can favour progression toward end-stage renal disease (Molitch *et al.,* 2004).

Several lines of evidence indicate that advanced glycation end products (AGEs), by exerting both direct (physico-chemical) and indirect (receptor-mediated) effects, have a major role in the development and progression of diabetic and non-diabetic renal disease. Receptor-independent effects include the modification of enzymatic activity, ligand binding, half-life and immunogenicity, whereas AGE binding to the advanced glycosylation end-product-specific receptor (**AGER**) triggers redox-sensitive signalling pathways leading to tissue injury *via* induction of apoptosis, inflammation and fibrosis (Bohlender *et al.,* 2005). AGEs accumulate in sera and tissues of subjects suffering from diabetes and also of those with dyslipidaemia, arterial hypertension and other disease conditions (Ahmed, 2005). Accumulation of these by-products is mainly due to increased formation of reactive carbonyl species (RCS) derived from oxidation and also from non-oxidative metabolism of carbohydrates and lipids, of which there is an overabundance in patients with type 2 diabetes (Negre-Salvayre *et al.,* 2008). In turn, RCS, which include the α-oxoaldehyde glyoxal and the aldehyde **4-hydroxynonenal (HNE)**, react with aminoacid residues on proteins to generate stable adducts and cross links collectively termed as AGEs (Ahmed, 2005; Ellis, 2007; Negre-Salvayre *et al.,* 2008).

Carnosine (β-alanyl-L-histidine) is an endogenous histidine-containing dipeptide that acts as a quencher of RCS (Aldini *et al.,* 2005), thus inhibiting AGE formation. L-Carnosine has been shown to be effective in several disease models in which carbonyl stress is thought to play a central pathogenic role, such as ischaemic and/or toxic injury of the kidney (Kurata *et al.,* 2006; Soliman *et al.,* 2007), lung (Cuzzocrea *et al.,* 2007) and brain (Rajanikant *et al.,* 2007; Tang *et al.,* 2007). In addition, L-carnosine was shown to protect kidney cells from the toxic effect of high glucose (Köppel *et al.,* 2011). Unfortunately, in humans, L-carnosine has a short half-life, due to its rapid inactivation by serum and tissue carnosinases [carnosine dipeptidases (CNDP)]. Recently, Ahluwalia *et al.* (2011) have shown that common variants in two CNDP genes (***CNDP1*** and ***CNDP2***) play a role in susceptibility to kidney disease in patients with type 2 diabetes. What is more, an experimental study conducted in *db*/*db* mice revealed that renal CNDP1 activity is up-regulated by post-translational modifications induced by RCS and ROS. In turn, increased CNDP1 activity reduces the availability of histidine-containing dipeptides in the diabetic kidney, thus establishing a positive feedback loop resulting in increasing renal carbonyl stress (Peters *et al.,* 2015). Therefore, the search for carnosinase-resistant carnosine derivatives represents a suitable strategy against carbonyl stress-dependent disorders. In particular, the vascular and renal complications associated with diabetes may benefit from treatment with these compounds to prevent both long-term glucose toxicity, resulting from insufficient glucose-lowering therapy, and lipotoxicity. Accordingly, the carnosinase-resistant D-carnosine pro-drug, D-carnosine-octylester (Vistoli *et al.,* 2009), was shown to be effective in attenuating experimental atherosclerosis and renal disease induced by a western diet or streptozotocin-induced diabetes in the ApoE-null mice (Menini *et al.,* 2012; 2015).

The aim of the present study was to investigate the effect of carnosinol, that is, (2S)-2-(3-amino propanoylamino)-3-(1H-imidazol-5-yl)propanol (FL-926-16), a newly synthesized L-carnosine derivative, on the onset and progression of diabetic nephropathy. To this end, we used the *db*/*db* mouse, a well-characterized model of type 2 diabetes and nephropathy, in which renal CNDP1 over-activity has been recently recognized (Peters *et al.,* 2015). An additional objective was to investigate the mechanism by which FL-926-16 exerts its effect by the use of primary cultures of mouse mesangial cells. The carnosine peptidomimetic FL-926-16 is selective and reactive as an RCS sequestering agent. In addition, it is characterized by a lack of toxicity and a favourable pharmacokinetic profile, related to its recognition by human peptide transporter 1 as well as resistance to carnosinase (Negrisoli *et al.,* 2011) and, hence, is not affected by changes in CNDP1 activity (Peters *et al.,* 2015).

Methods

Design

Animal studies are reported in compliance with the ARRIVE guidelines (Kilkenny *et al.*, 2010; McGrath and Lilley, 2015).

In vivo studies

Randomization and treatment. In this study, C57BLKS/J^{Lepr} male 6-week-old diabetic *db*/*db* and control *db*/*m* mice were used (see Results for body weights and blood glucose levels at baseline). The *db*/*db* mouse is one of the best characterized and most investigated model of diabetic nephropathy (Sharma *et al.,* 2003). Mice were assigned to blocks based on genotype and, within each block, randomized to receive no treatment (Ctrl and Diab, respectively) or FL-926-16 at a dose of 30 mg·kg^{-1}·day^{-1} in the drinking water (Ctrl-FL and Diab-FL, respectively). The dose of 30 mg·kg^{-1}·day^{-1}was chosen on the basis of results from preliminary *in vivo* and *in vitro* studies (Negrisoli *et al.,* 2011; Anderson EJ *et al*, unpublished observations) indicating a good safety profile of the compound and a good oral bioavailability, giving a significant exposure in plasma after oral administration at the dose ranging from 10 to 45 mg·kg^{-1}·day^{-1}. In the prevention protocol, FL-926-16 therapy was started at week 6, that is, prior to the onset of diabetic nephropathy, and ended at week 20, whereas in the

regression protocol, treatment was started at week 20, that is, after the onset of diabetic nephropathy, and ended at week 34.

Group sizes and ethical approval. The study was designed and started in 2014, that is, before power analysis for establishing group size in experimental research was a requirement. The group sizes were established on the basis of previous studies (Pugliese *et al.,* 2000; Iacobini *et al.,* 2004; 2009a; Menini *et al.,* 2007; Solini *et al.,* 2013) indicating that five animals per group provide sufficient power for detecting significant differences in functional (total proteinuria) and structural [fractional mesangial area (fMA)] parameters in experimental settings of diabetic nephropathy. However, in the prevention protocol, since other outcomes were evaluated in addition to renal function and structure in order to get mechanistic insights, the number of mice for each group was doubled (10 animals). The study protocol was approved by the ethical committee of the Catholic University of Rome, Italy (no. 355/2008). The animals were housed in single cages with wood-derived bedding material in a specific pathogen-free facility with a 12 h light/dark cycle and in controlled temperatures (20–22°C). Mice were cared for in accordance with the Principles of Laboratory Animal Care (National Institutes of Health publ. no. 85-23, revised 1985) and with national laws and received water and food *ad libitum*. At the end of the study periods, mice were placed into metabolic cages overnight to collect urine. The next day, body weights were recorded, then mice were anaesthetised with ketamine (60 $mg \cdot kg^{-1}$ Imalgene i.p.) and xylazine (7.5 $mg \cdot kg^{-1}$ Rompum i.p.), as established by the veterinarian of the facility, and a blood sample was obtained by cardiac puncture. Finally, the animals were killed by cervical dislocation, a longitudinal incision of the abdominal wall was performed, and both kidneys were quickly removed and weighed. All the measurements indicated below were performed in the prevention protocol, whereas only metabolic parameters, renal function and structure, and markers of systemic oxidative and carbonyl stress were analysed in the regression protocol. No animal losses occurred, and all animals were used for the analysis of metabolic parameters, kidney weight and renal function and structure, whereas five animals per group, randomly selected, were used for immunohistochemistry (IHC) and quantitative RT-PCR (qRT-PCR). All the analyses were performed by investigators blinded to group assignment. To this end, biological samples were recoded by a technician (C.C., see Acknowledgements) at the time of collection.

In vitro studies

Mesangial cells were isolated from male C57BL6 mice as previously described (Pugliese *et al.,* 2000). Cells between the 3rd and the 10th passage were cultured in DMEM supplemented with 10% FBS, 2 $mmol \cdot L^{-1}$ L-glutamine, and antibiotics at 37°C in a 95% air/5% CO_2-humidified atmosphere. Cells were incubated for 24 h with saline, N^{ε}-carboxymethyllysine (CML, 100 $\mu g \cdot mL^{-1}$), its dialdehyde precursor, the RCS glyoxal (100 μM) or the lipoxidation-derived RCS HNE (5 μM), in the presence or absence of FL-926-16 (20 mM) (Menini *et al.,* 2012).

Monolayers were then collected, and total RNA was extracted to assess the gene expression of the gene for **NOD-like receptor family, pyrin domain containing 3 (NLRP3)** inflammasome (*Nlrp3*), which was previously shown to participate in renal inflammation and injury in an animal model of metabolic syndrome (Solini *et al.,* 2013).

All experiments were conducted five times in triplicate; technical replicates were used to ensure the reliability of single values.

Measurements

Metabolic parameters. Blood glucose levels were measured with the aid of the automated colorimetric instrument Glucocard™, whereas serum insulin levels were assessed by an ELISA kit.

The Homeostasis Model of Assessment – Insulin Resistance index was then calculated from glucose and insulin levels.

Total cholesterol and triglycerides were assessed by enzymatic colorimetric methods.

Renal function. Serum and urine creatinine levels were measured by HPLC, whereas total proteinuria was assessed by the Bradford method and albuminuria by ELISA.

Values of proteinuria and albuminuria were normalized by the urine creatinine concentration and expressed as protein/creatinine (P/C) and albumin/creatinine (A/C) ratios respectively (Iacobini *et al.,* 2004).

Renal morphology/morphometry. For the analysis of renal structure (Iacobini *et al.,* 2004; Menini *et al.,* 2015), serial 4 μm kidney sections were stained with periodic acid Schiff (PAS). Then, the areas of at least 100 glomerular tuft profiles per sample were measured by means of the computer-assisted image analysis system Optimas 6.5 and expressed as mean glomerular area (mGA), and PAS-positive material in each glomerulus was quantified and expressed as percentage of the glomerular tuft area (fMA). Finally, the mean mesangial area (mMA) was calculated from the following formula: (fMA × mGA)/100.

Glomerular extracellular matrix and cell apoptosis. The mRNA expression of the genes for the extracellular matrix components **fibronectin (Fn1)** and **collagen IV α1 chain (Col4a1)** and the pro-fibrotic cytokine TGF-β (*Tgfβ*) were assessed by qRT-PCR using a StepOne™ RT-PCR instrument and TaqMan Gene Expression Assays, as previously reported (Menini *et al.,* 2007).

Briefly, total RNA was extracted from mice renal cortex and mesangial cells with the RNAeasy mini kit. Then, 1 μg of RNA was reverse-transcribed in a 20 μL reaction tube using a High Capacity cDNA Reverse Transcription Kit, and RT-PCR was performed in triplicate on a StepOne™ RT-PCR following the standard protocol. Transcripts for *Fn1, Col4a1* and *Tgfβ* were quantified by TaqMan Gene Expression Assays using the assays reported in Supporting Information Table S1.

Amplifications were normalized to the β-actin gene (*Actb*), and gene expression was quantified using the ΔΔCT calculation, where CT is the threshold cycle. The amount

of the target gene was expressed as fold of control mean (*db*/*m* controls or untreated cells) to control for unwanted sources of variation. A standard curve for each gene was constructed using multiple calibrator dilutions. Standard curves were accepted only if the slope was approximately −3, with an *r* value greater than 0.98, and were used to estimate PCR efficiency. Results were analysed using SDS 2.1 software.

Protein content and distribution of extracellular matrix were assessed by IHC using rabbit polyclonal antibodies to human fibronectin and mouse collagen IV α1 chain (Iacobini *et al.,* 2004; Menini *et al.,* 2007). As for PAS positivity, the percentage of the glomerular area with positive staining was calculated by means of the image analysis system Optimas™6.5. A region of interest was drawn around the glomerulus, then the percentage of positive area for the specific stain (purple-magenta for PAS and brown colour for IHC) was calculated at a fixed colour threshold, which was set by identifying three to five separate pixels in areas of positive staining. For each kidney specimen, the average of at least 60 glomeruli was used.

Protein levels of collagen IV α1 chain in homogenates of renal cortex were also assessed by Western blot using the same antibody utilized for IHC. As for mRNA expression levels, results are expressed as fold of control mean.

Glomerular cell death rate was assessed by IHC for active caspase-3 using a rabbit polyclonal antibody. Positive cells were counted and expressed as % of total cells (Iacobini *et al.,* 2004; Menini *et al.,* 2007). A custom-made, C-language macro was written to count the number of cells within each glomerular tuft profile by means of the Optimas™6.5 image analysis system. At least 60 glomerular tuft profiles per sample were measured.

Serum and renal markers of oxidative and carbonyl stress and FL-926-16 levels. Serum levels of isoprostane 8-epi-$PGF_{2\alpha}$, an index of systemic oxidative stress, were determined by ELISA using a commercial kit (Iacobini *et al.,* 2009a,b). Total carbonylated proteins (PCOs) were measured by slot blot immunoassay using an anti-dinitrophenylhydrazone antibody, after carbonyl derivatization with dinitrophenylhydrazine (Vistoli *et al.,* 2009; Orioli *et al.,* 2011); serum AGE levels by a competitive ELISA technique (Menini *et al.,* 2007; Iacobini *et al.,* 2009a); serum pentosidine levels by HPLC (Odetti *et al.,* 1992); and FL-926-16 concentrations in serum and urine by LC-ESI-MS/MS (MRM mode) (Anderson EJ *et al.*, unpublished observations). The tissue content of CML, a glyoxal-derived protein adduct, HNE histidine adduct (Michael adduct), AGER and the renal isoform of NAD(P)H oxidase (Nox4) were assessed by IHC (see above), using a biotinylated mouse monoclonal antibody against CML, a rabbit antiserum against the HNE protein adduct, a goat polyclonal antibody to AGER and a rabbit monoclonal antibody to Nox4 respectively (Iacobini *et al.,* 2009a,b).

Renal inflammation. The mRNA expression of the genes for TNF-α (*Tnfa*), monocyte chemoattractant protein-1 (**MCP-1, Mcp1; also known as CCL2**), the monocyte/macrophage cell marker Cell surface glycoprotein **F4/80** or **adhesion GPCR E1 (Adgre1)** and of the NLRP3 inflammasome (*Nlrp3*) were assessed by qRT-PCR (Iacobini *et al.,* 2009a,b; Solini *et al.,* 2013).

Protein content and distribution of F4/80, MCP-1 and NLRP3 were assessed by IHC (see above), using a rat monoclonal antibody to mouse F4/80 and rabbit polyclonal antibodies to MCP-1 and NLRP3 (Solini *et al.,* 2013). For F4/80 and MCP-1, positive staining was measured in 20 random fields of the renal cortex examined at a final magnification of 400× and expressed as the mean percentage of field area occupied by the specific stain.

Finally, protein levels of F4/80 in homogenates of renal cortex were also assessed by Western blot using the same antibody utilized for IHC.

Statistical analysis

The data and statistical analysis comply with the recommendations on experimental design and analysis in pharmacology (Curtis *et al.,* 2015).

Results are expressed as mean ± SD and % change versus controls.

Statistical significance was evaluated by Student's *t*-test or one-way ANOVA followed by the Bonferroni test for multiple comparisons. For variables not normally distributed, the Kruskal–Wallis test was applied, followed by the Mann–Whitney *U*-test for pairwise comparisons. The *post hoc* tests were run only if F achieved $P < 0.05$ and there was no significant variance inhomogeneity.

A *P*-value <0.05 was considered significant. All statistical tests were performed on raw data using the SPSS version 13.0 (SPSS Inc., Chicago, IL, USA).

Materials

The *db*/*db*, *db*/*m* and C57BL6 mice were purchased from Charles River (Calco, Italy). The study drug FL-926-16 was obtained from Flamma S.p.A. (Chignolo d'Isola, Italy).

DMEM, mouse serum albumin, glyoxylic acid, sodium cyanoborohydrate, glyoxal and antibodies to human fibronectin and NLRP3 (HPA012878) were purchased from Sigma (St. Louis, MO, USA); FBS, L-glutamine and antibiotics from Flow Laboratories (Irvine, Scotland, UK); the ELISA kit for insulin from Mercodia AB (Uppsala, Sweden); the enzymatic colorimetric kit for total cholesterol and triglycerides from Roche Diagnostics (Milan, Italy); the Bradford dye-binding protein assay kit from Pierce (Rockford, IL, USA); the Mouse Albumin ELISA Quantification Kit from Bethyl (Montgomery, TX, USA); the RNAeasy mini kit from Qiagen (Milan, Italy); HNE and the ELISA kit for 8-epi- $PGF_{2\alpha}$ from Cayman (Ann Arbor, MI, USA); the High Capacity cDNA Reverse Transcription Kit and TaqMan Gene Expression Assays from Applied Biosystems (Monza, Italy); the antibodies to mouse collagen IV α1 chain (IHC and western blot), Nox4 (UOTR1B492), F4/80 (IHC and western blot) and MCP-1 from Abcam (Cambridge, UK); the Anti-ACTIVE® caspase-3 antibody from Promega Italia (Milan, Italy); the antibody against CML from Wako (Neuss, Germany); the antibody against the HNE protein adduct from Alpha Diagnostic International (San Antonio, TX, USA); and the antibody to AGER (ab7764) from Novus Biologicals (Littleton, CO, USA).

As previously reported (Iacobini *et al.,* 2011), CML was prepared by incubating 175 mg mouse serum albumin in 1 mL of 0.2 M phosphate buffer, pH 7.8, containing 0.15 M

Table 1

Metabolic parameters, kidney weight and renal function

	Ctrl	Ctrl-FL-926-16	Diab	Diab-FL-926-16
Body weight, g	30.2 ± 1.2	30.0 ± 2.1	46.2 ± 4.8*	46.1 ± 3.9*
Glucose, mmol·L^{-1}	7.85 ± 1.02	7.80 ± 1.40	25.18 ± 4.78*	25.24 ± 5.11*
Insulin, pmol·L^{-1}	77.6 ± 17.2	78.2 ± 9.5	287.6 ± 30.3*	278.4 ± 31.2*
HOMA-IR	3.80 ± 0.77	3.78 ± 0.76	46.19 ± 9.59*	41.60 ± 9.25*
Cholesterol, mmol·L^{-1}	1.88 ± 0.43	1.86 ± 0.43	3.27 ± 0.30*	3.23 ± 0.37*
Triglycerides, mmol·L^{-1}	0.69 ± 0.13	0.70 ± 0.12	1.04 ± 0.11*	1.01 ± 0.15*
8-epi-PGF$_{2\omega}$, pg·mL^{-1}	65.0 ± 6.52	62.4 ± 12.5	146.8 ± 14.4*	75.8 ± 10.8†
PCOs, pmol·mg·prot^{-1}	1.50 ± 0.27	1.47 ± 0.24	2.90 ± 0.61*	1.55 ± 0.16†
AGEs, U·mL^{-1}	3.98 ± 1.14	3.78 ± 0.82	9.27 ± 1.23*	5.31 ± 0.84†
Pentosidine, pg·mL^{-1}	53.1 ± 2.8	51.8 ± 5.3	117.4 ± 10.4*	71.4 ± 8.1†
P-FL-926-16, μmol·L^{-1}	0.00 ± 0.00	0.21 ± 0.07†	0.00 ± 0.00	0.22 ± 0.04†
U-FL-926-16, μmol·L^{-1}	0.00 ± 0.00	37.09 ± 6.46†	0.00 ± 0.00	16.83 ± 2.50*†
Kidney weight, mg	217.7 ± 35.9	213.8 ± 33.1	253.8 ± 18.5*	241.5 ± 20.8
Creatinine, μmol·L^{-1}	30.5 ± 2.4	30.1 ± 1.7	51.3 ± 7.1*	34.7 ± 2.3†
Urinary P/C, mg·g^{-1}	1.86 ± 0.51	1.89 ± 0.25	35.68 ± 7.88*	10.26 ± 1.93*†
Urinary A/C, mg·g^{-1}	1.28 ± 0.34	1.24 ± 0.25	25.72 ± 7.52*	6.90 ± 1.68*†

Values of untreated and FL-926-16-treated *db*/*m* and *db*/*db* mice at 20 weeks of age (prevention protocol; $n = 10$ per group).
Kidney weight refers to both kidneys. HOMA-IR, Homeostasis Model of Assessment – Insulin Resistance; N/A, not assessed; *Post hoc* multiple comparison:
*$P < 0.05$ versus Ctrl;
†$P < 0.05$ versus Diab.

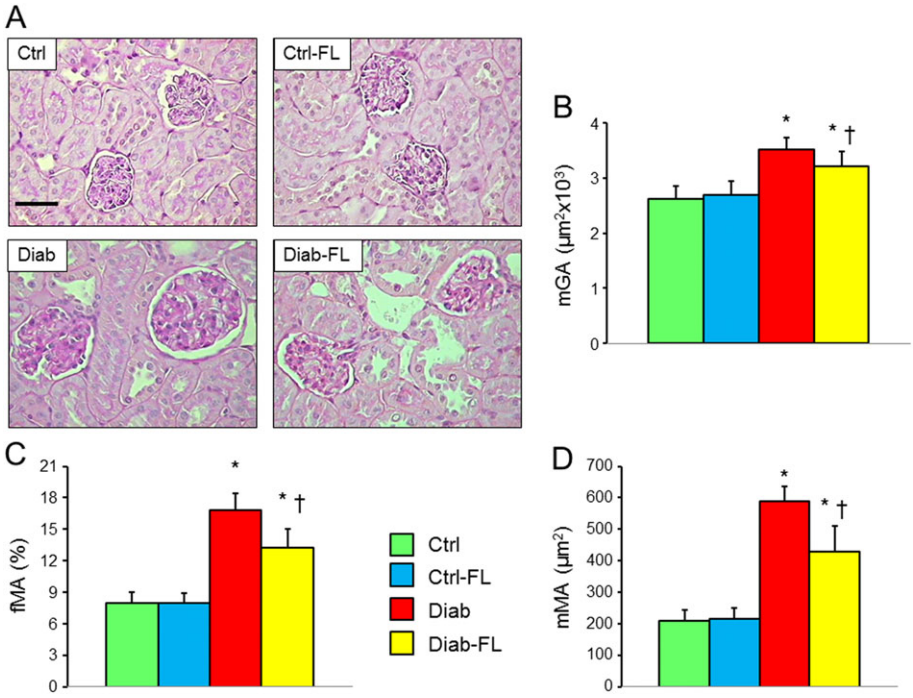

Figure 1

Prevention protocol: renal structure. PAS staining of kidney sections from representative animals (A) and quantification of mGA (B), fMA (C) and mMA (D) in untreated and FL-926-16 (FL)-treated *db*/*m* control (Ctrl) and *db*/*db* diabetic (Diab) mice (mean ± SD; $n = 10$ per group). Scale bar = 50 μm. *Post hoc* multiple comparison: *$P < 0.05$ versus Ctrl; †$P < 0.05$ versus Diab.

glyoxylic acid and 0.45 M sodium cyanoborohydrate for 24 h at 37°C.

The instrument for blood glucose measurement Glucocard™ SM was from A.Menarini Diagnostics (Florence, Italy); the image analysis system Optimas 6.5 was from Bioscan (Washington DC, USA); the StepOne™ RT-PCR instrument was from Thermo Fisher Scientific (Monza, Italy); and the SDS 2.1 software was from Applied Biosystem.

Nomenclature of targets and ligands

Key protein targets and ligands in this article are hyperlinked to corresponding entries in http://www.guidetopharmacology.org, the common portal for data from the IUPHAR/BPS Guide to PHARMACOLOGY (Southan *et al.*, 2016), and are permanently archived in the Concise Guide to PHARMACOLOGY 2017/18 (Alexander *et al.*, 2017a,b,c).

Results

In vivo studies

Baseline body weights and blood glucose levels in Ctrl and Diab mice were 20.2 ± 1.4 and 23.3 ± 2.7 g and 6.57 ± 1.02 and 9.50 ± 2.67 mmol·L^{-1} respectively.

Prevention protocol

Metabolic parameters. Growth impairment and metabolic derangement were similar in Diab versus Ctrl mice and were not affected by FL-926-16 treatment (Table 1).

Renal function. Serum creatinine increased significantly in Diab mice, and these increases were significantly reduced in Diab-FL animals; values from Diab-FL mice did not differ from those of Ctrl mice. Likewise, A/C and P/C ratios increased significantly in Diab mice, and these increments were markedly attenuated in Diab-FL animals, although values remained significantly higher than in Ctrl mice (Table 1).

Renal structure. Kidney weights increased significantly versus Ctrl mice in untreated but not in FL-926-16-treated Diab animals (Table 1). Moreover, mGA, mMA and fMA were significantly higher in Diab than in Ctrl mice, and increases were significantly reduced, but not normalized, in Diab-FL animals (Figure 1), indicating that treatment largely prevented glomerular lesions. Consistent with previous observations in *db*/*db* mice (Sharma *et al.*, 2003), no expansion of the tubule-interstitium was observed in Diab animals.

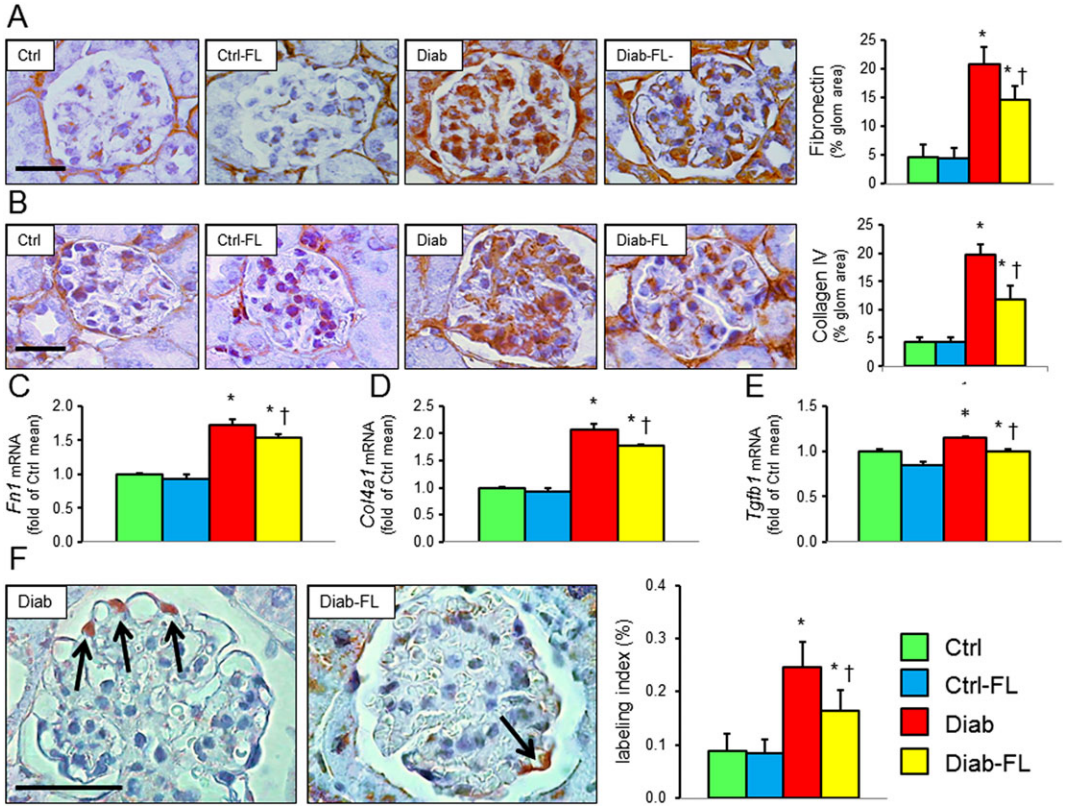

Figure 2

Prevention protocol: glomerular extracellular matrix and cell apoptosis. IHC of kidney sections from representative animals and quantification of fibronectin (A) and collagen IV α1 chain (B); kidney mRNA expression of *FN1* (C), *Col4a1* (D) and *Tgfb* (E); IHC of kidney sections (original quantification 1000×) from representative animals and quantification of active caspase-3 (F, arrows indicate positive cells) in untreated and FL-926-16 (FL)-treated *db*/*m* control (Ctrl) and *db*/*db* diabetic (Diab) mice (mean ± SD; $n = 5$ per group). Scale bar = 50 μm. *Post hoc* multiple comparison: *$P < 0.05$ versus Ctrl; †$P < 0.05$ versus Diab.

Glomerular extracellular matrix and cell apoptosis. At IHC, the glomerular concentration of the extracellular matrix proteins fibronectin and collagen IV was significantly higher in Diab versus Ctrl mice and was significantly reduced, but not normalized, in Diab-FL versus Diab mice (Figure 2A, B). Similar findings were observed for kidney cortex transcripts of *Fn1*, *Col1a1* and *Tgfb* (Figure 2C–E) and for kidney cortex protein levels of collagen IV, as assessed by Western blot (Supporting Information Figure S1). The number of glomerular cells positive for active caspase-3 was very low in Ctrl animals and increased significantly in Diab animals, with a predominant involvement of podocytes, although mesangial and endothelial cells were also affected. Once again, these increases in apoptosis were significantly attenuated, but not prevented, in Diab-FL mice (Figure 2F).

Systemic and renal oxidative and carbonyl stress and FL-926-16 levels. Circulating levels of isoprostane 8-epi-$PGF_{2\alpha}$, PCOs

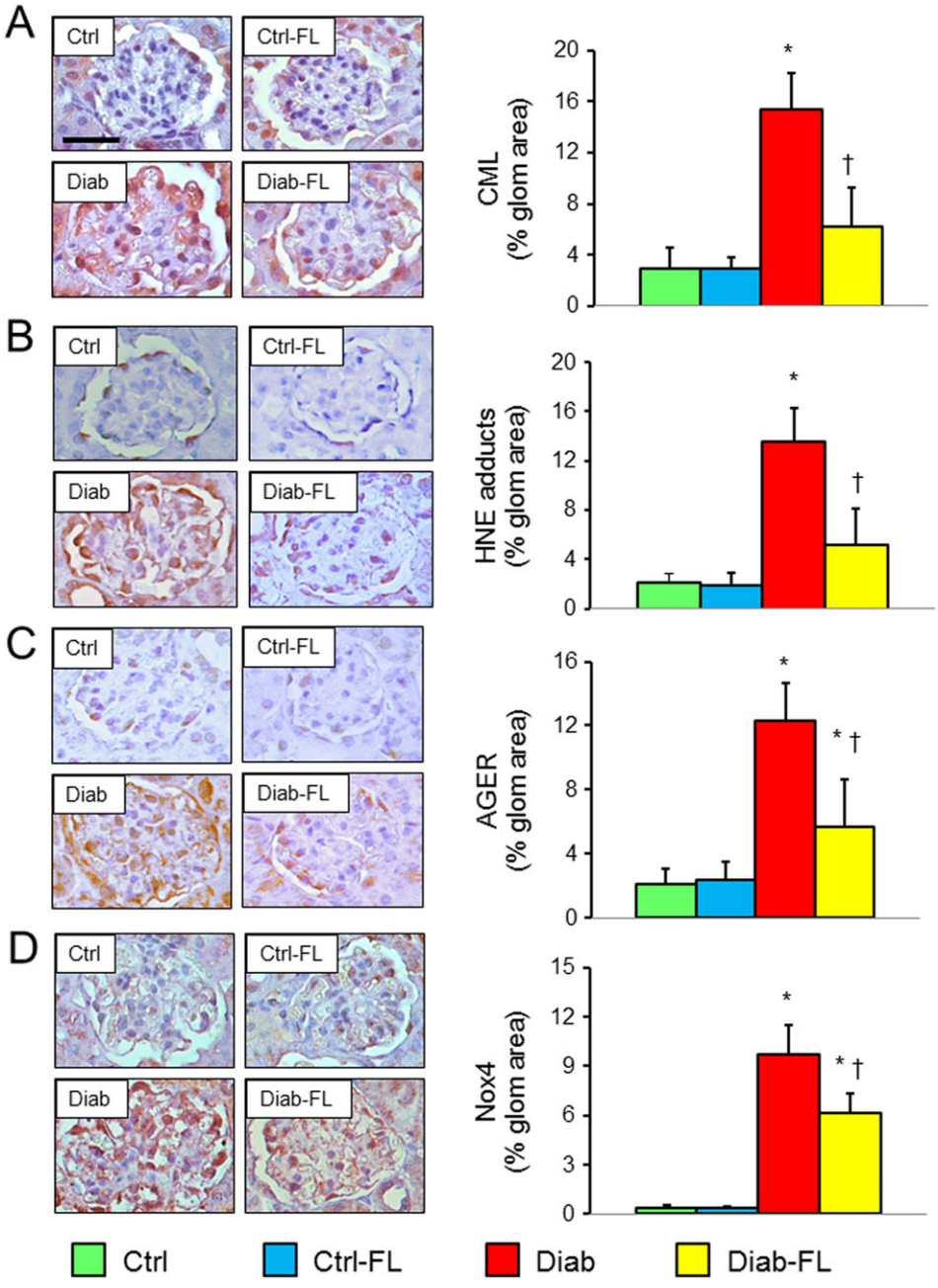

Figure 3

Prevention protocol: renal oxidative and carbonyl stress. IHC of kidney sections from representative animals and quantification of CML (A), HNE (B), AGER (C) and Nox4 (D) in untreated and FL-926-16 (FL)-treated *db*/*m* control (Ctrl) and *db*/*db* diabetic (Diab) mice (mean ± SD; $n = 5$ per group). Scale bar = 50 μm. *Post hoc* multiple comparison: *$P < 0.05$ versus Ctrl; †$P < 0.05$ versus Diab.

and AGEs were increased in Diab versus Ctrl mice and reduced by FL-926-16 treatment to values that did not differ significantly from those of Ctrl animals. A similar trend was observed for pentosidine (Table 1). Glomerular staining for CML and HNE adducts was slightly positive in Ctrl mice and increased significantly in Diab mice. Increases were significantly attenuated in Diab-FL animals, which showed values that did not differ from those of Ctrl mice for CML and HNE adducts (Figure 3A, B). Also immunostaining for AGER and Nox4, which was minimal in glomeruli from Ctrl animals, increased significantly in Diab, and these increases were markedly reduced in Diab-FL mice (Figure 3C, D). FL-926-16 was detected only in the plasma and urine from treated animals, with lower urinary levels in Diab versus Ctrl mice, probably due to the reduced renal function and/or increased FL-926-16-RCS formation (Table 1).

Renal inflammation. At IHC, the renal concentrations of the inflammatory markers F4/80 and MCP-1 were markedly increased in Diab mice and these increases were significantly attenuated in Diab-FL animals, which showed a level of positivity similar to that of Ctrl mice (Figure 4A, B). Similar findings were observed for protein levels of F4/80 in renal cortex homogenates, as evaluated by Western blot analysis (Supporting Information Figure S1). Likewise, tubular staining for NLRP3, which was insignificant in both Ctrl and Ctrl-FL mice, increased significantly in Diab animals and also showed a strong positivity of glomerular cells but not in Diab-FL mice (Figure 5A). Renal cortex mRNA levels of *Adgre1*, *Mcp1*, *Tnfa* (Figure 4C–E) and *Nlrp3* (Figure 5B) were significantly increased in Diab mice, and these changes were significantly attenuated by FL-926-16 treatment, although Diab-FL animals still exhibited higher values than Ctrl mice.

Regression protocol

Metabolic parameters. As in the prevention protocol, FL-926-16 treatment did not affect the growth impairments and metabolic derangement in Diab mice (Table 2).

Renal function. In the regression protocol, the increases in serum creatinine as well as in A/C and P/C ratios in Diab mice were also significantly reduced by FL-926-16 treatment, although values remained significantly higher than in Ctrl mice. Interestingly, as compared with 20-week-

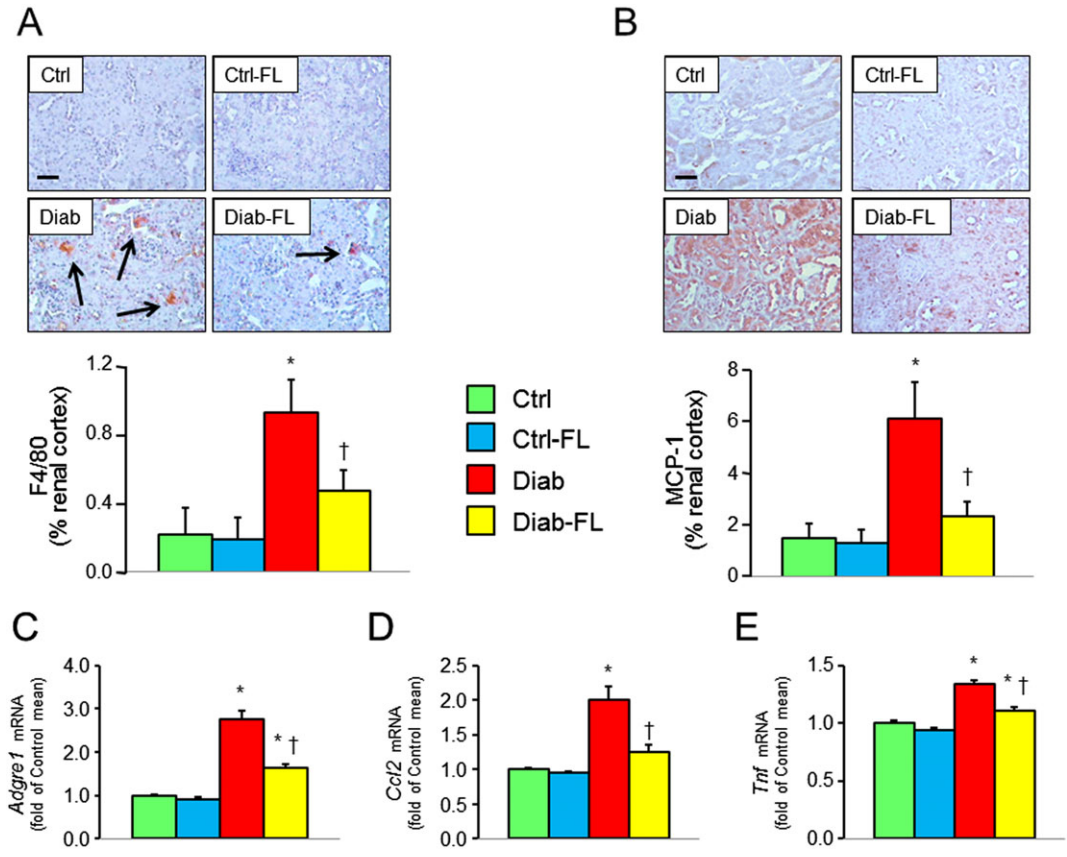

Figure 4

Prevention protocol: renal inflammation. IHC of kidney sections from representative animals and quantification of F4/80 (A) and MCP-1 (B) and kidney mRNA expression of *Adgre1* (C), *Mcp1* (D) and *Tnfa* (E) in untreated and FL-926-16 (FL)-treated *db*/*m* control (Ctrl) and *db*/*db* diabetic (Diab) mice (mean ± SD; $n = 5$ per group). Scale bar = 50 μm. *Post hoc* multiple comparison: *$P < 0.05$ versus Ctrl, †$P < 0.05$ versus Diab.

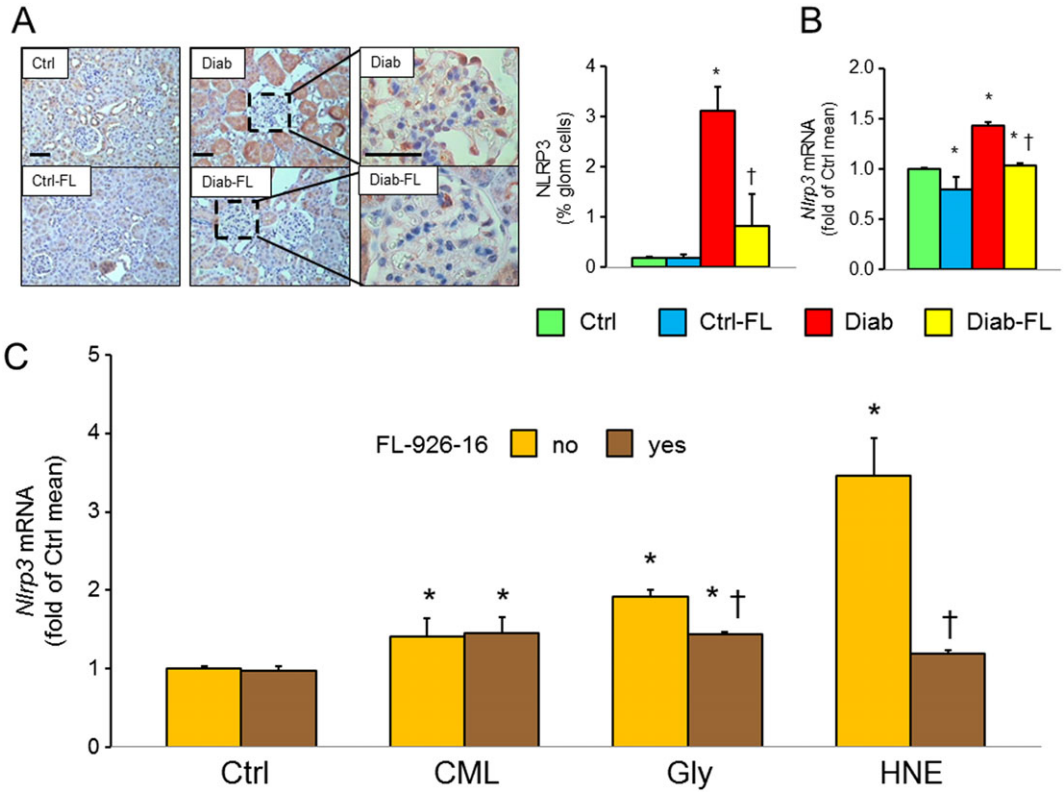

Figure 5

In vivo and *in vitro* studies: NLRP3 expression. IHC of kidney sections from representative animals and quantification of NLRP3 (A) and kidney mRNA expression of *Nlrp3* (B) in untreated and FL-926-16 (FL)-treated *db*/*m* control (Ctrl) and *db*/*db* diabetic (Diab) mice (mean ± SD; $n = 5$ per group). Scale bar = 50 μm. *Post hoc* multiple comparison: *$P < 0.05$ versus Ctrl; †$P < 0.001$ versus Diab. Expression levels of *Nlrp3* in mouse mesangial cells incubated with vehicle (Ctrl), 100 $\mu g \cdot mL^{-1}$ CML, 100 μM glyoxal (Gly) or 5 μM HNE, without and with FL-926-16 20 mM (C) (mean ± SD; $n = 5$ experiments in triplicate). Pairwise comparison: *$P < 0.05$ versus Ctrl; †$P < 0.05$ versus untreated.

old Diab mice, levels were higher in 34-week-old Diab ($P < 0.05$), but not Diab-FL mice, indicating that the progression of renal dysfunction was blocked by initiation of FL-926-16 treatment (Table 2).

Renal structure. Kidney weights increased significantly versus Ctrl mice in untreated but not in FL-926-16-treated Diab animals also in the regression protocol (Table 2). The increases in mGA, mMA and fMA (Figure 6) observed in Diab animals were significantly reduced but not normalized in Diab-FL animals. When compared with those of 20-week-old untreated Diab animals, changes in the structural parameters were significantly higher in untreated Diab mice but not in FL-926-16-treated at 34 weeks of age, thus indicating that progression was halted by FL-926-16 treatment, although it did not cause significant regression (Figure 7).

Systemic oxidative and carbonyl stress. Also in the regression protocol, the increased levels of isoprostane 8-epi-$PGF_{2\alpha}$, PCOs and AGEs observed in Diab mice were reduced by FL-926-16 treatment to values similar to those of Ctrl animals (Table 2).

In vitro studies

The RCSs glyoxal and HNE and the glyoxal-derived protein adduct CML induced the mRNA expression of *Nlrp3* in mesangial cells. FL-926-16 completely prevented HNE-induced *Nlrp3* up-regulation and significantly attenuated glyoxal-induced *Nlrp3* up-regulation but was not able to inhibit *Nlrp3* expression induced by CML (Figure 5C).

Discussion

In view of the key role of AGE accumulation in the pathogenesis of diabetic nephropathy (Wendt *et al.*, 2003; Cooper, 2004), therapeutic strategies aimed at reducing AGE-induced tissue injury have been proposed and tested in experimental animals (Bakris *et al.*, 2004; Reddy and Beyaz, 2006). Some of these agents have also been investigated in humans with inconclusive results, due to safety concerns and inconsistent efficacy, possibly due to the advanced degree of disease progression in patients enrolled in these studies (Cooper, 2004). The AGE-reducing strategies inhibit the formation of AGEs by quenching their precursors, RCS, with carbonyl scavengers, which include histidine-containing dipeptides (Ellis, 2007).

Table 2

Metabolic parameters, kidney weight and renal function

	Ctrl	Ctrl-FL-926-16	Diab	Diab-FL-926-16
Body weight, g	34.5 ± 3.0	33.8 ± 1.7	45.5 ± 2.0*	45.6 ± 7.6*
Glucose, mmol·L^{-1}	9.18 ± 0.43	9.11 ± 0.63	29.74 ± 2.43*	28.95 ± 2.38*
Insulin, pmol·L^{-1}	72.6 ± 8.1	73.0 ± 10.5	254.4 ± 18.8*	251.3 ± 15.6*
HOMA-IR	4.27 ± 0.51	4.23 ± 0.49	48.20 ± 1.81*	46.39 ± 1.91*
Cholesterol, mmol·L^{-1}	1.98 ± 0.24	1.98 ± 0.15	3.80 ± 0.41*	3.81 ± 0.40*
Triglycerides, mmol·L^{-1}	0.76 ± 0.10	0.77 ± 0.07	1.09 ± 0.10*	1.06 ± 0.10*
8-epi-PGF$_{2\omega}$, pg·mL^{-1}	71.0 ± 4.7	70.4 ± 2.4	165.6 ± 8.8*	77.6 ± 13.3†
PCOs, pmol·mg·prot^{-1}	1.57 ± 0.06	1.56 ± 0.13	3.12 ± 0.34*	1.94 ± 0.16†
AGEs, U·mL^{-1}	5.37 ± 0.64	4.94 ± 0.83	10.57 ± 1.30*	6.67 ± 1.09†
Pentosidine, pg·mL^{-1}	N/A	N/A	N/A	N/A
P-FL-926-16, µmol·L^{-1}	N/A	N/A	N/A	N/A
U-FL-926-16, µmol·L^{1}	N/A	N/A	N/A	N/A
Kidney weight, mg	234.0 ± 19.5	232.0 ± 14.8	278.0 ± 14.8*	256.0 ± 11.4
Creatinine, µmol·L^{-1}	31.5 ± 1.3	31.3 ± 1.6	62.1 ± 6.4*	50.7 ± 5.9*†
Urinary P/C, mg·g^{-1}	2.03 ± 0.32	2.08 ± 0.09	44.65 ± 7.89*	28.04 ± 4.84*†
Urinary A/C, mg·g^{-1}	1.42 ± 0.23	1.43 ± 0.22	33.48 ± 4.96*	19.65 ± 2.63*†

Values of untreated and FL-926-16-treated *db*/*m* and *db*/*db* mice at 34 weeks of age (regression protocol; $n = 5$ per group).
Kidney weight refers to both kidneys. HOMA-IR, Homeostasis Model of Assessment – Insulin Resistance; N/A, not assessed; *Post hoc* multiple comparison:
*$P < 0.05$ versus Ctrl;
$^{\dagger}P < 0.05$ versus Diab.

In the present study, we evaluated a novel carnosine peptidomimetic, FL-926-16, in the prevention/attenuation of the onset of diabetic nephropathy and the halting/regression of established diabetic nephropathy in *db*/*db* mice, a model of type 2 diabetes. These mice carry a G-to-T point mutation of the leptin receptor that causes polyphagia, obesity and insulin resistance followed by frank hyperglycaemia (by 4–6 weeks of age) and renal features resembling those of human diabetic nephropathy (Sharma *et al.*, 2003). The main finding of our study was that treatment with FL-926-16 significantly reduced the changes in renal function and structure occurring in *db*/*db* mice. Importantly, FL-926-16 treatment was effective both in attenuating the onset of diabetic nephropathy and in stopping its progression. This was demonstrated by the markedly reduced increment in serum creatinine, albuminuria, total proteinuria, glomerular hypertrophy and mesangial expansion, as compared with age-matched, untreated *db*/*db* mice. Of note, these differences in the severity of renal involvement between the two diabetic groups occurred despite similar degrees of metabolic derangement. This observation is at variance with previous studies showing an improvement in glucose homeostasis in *db*/*db* mice treated with L-carnosine (Block *et al.*, 2009; Gorin *et al.*, 2015).

The glomeruli of *db*/*db* mice underwent significant remodelling, as indicated by fibronectin and collagen IV accumulation and increased glomerular cell apoptosis. These changes were associated with increased serum levels of isoprostane 8-epi-PGF$_{2\alpha}$, PCOs and AGEs, augmented glomerular content of AGEs and their receptor AGER and markedly increased Nox4 expression, the major NADPH oxidase renal isoform involved in ROS production and diabetes-associated kidney damage (Block *et al.*, 2009; Gorin *et al.*, 2015). In addition, kidneys of *db*/*db* mice showed signs of inflammation, as demonstrated by the increased protein levels of F4/80 and transcripts for *Adgre1*, *Mcp1* and *Tnfa*. Interestingly, the NLRP3 inflammasome, which has been recently shown to serve as a central mechanism in the pathogenesis of type 2 diabetes-associated renal inflammation and injury (Anders and Muruve, 2011; Solini *et al.*, 2013), was also markedly increased in renal tissue of *db*/*db* mice, at both the protein and mRNA level. The elevation of all these parameters was markedly blunted in *db*/*db* mice treated with FL-926-16, in which a reduction in systemic and renal carbonyl and oxidative stress was associated with attenuated renal/glomerular fibrosis, apoptosis and inflammation.

These data provide further insights into the mechanisms underlying the injurious effect of AGEs in diabetic nephropathy as well as the favourable action of carnosine derivatives on this disorder. In fact, FL-926-16 was very effective in blunting the diabetes-induced up-regulation of the NLRP3 inflammasome, thus suggesting that the pro-inflammatory response of the innate immune system triggered by AGEs involves the activation of this danger recognition platform, possibly *via* ROS generation (Anders and Muruve, 2011; Solini *et al.*, 2013). In addition, mesangial cells treated with FL-926-16 showed no or significantly attenuated RCS-induced *Nlrp3* expression, thus supporting the concept that

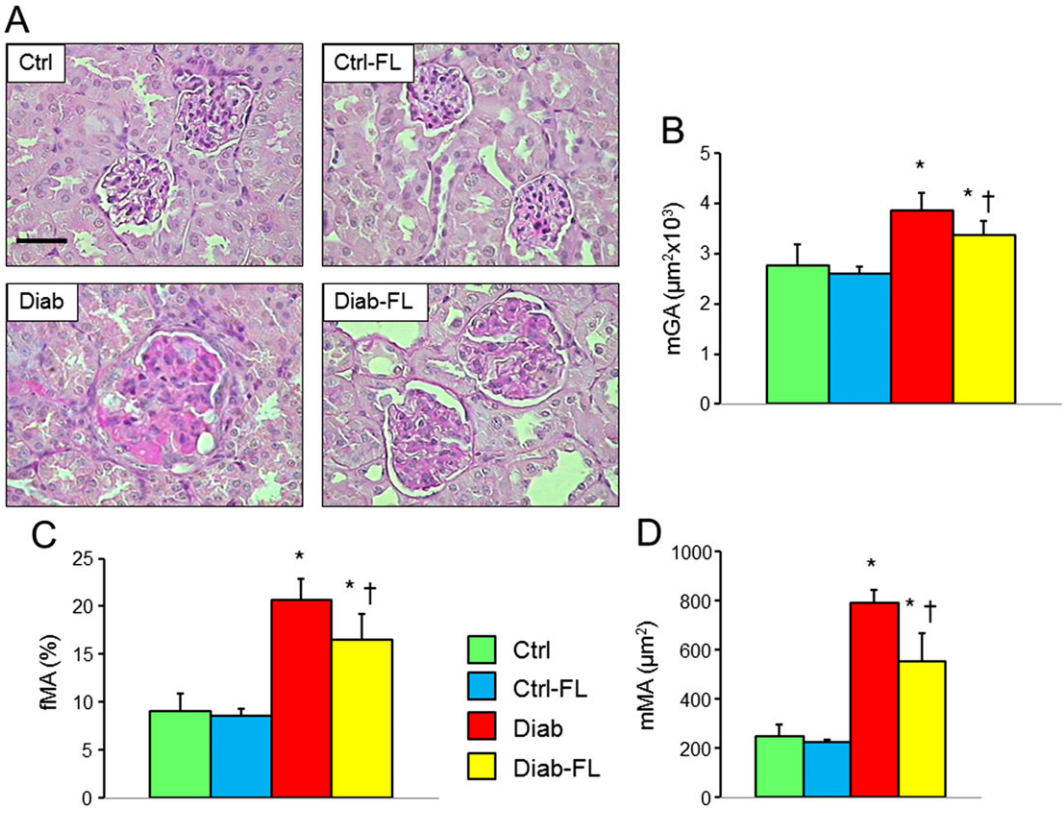

Figure 6

Regression protocol: renal structure. PAS staining of kidney sections from representative animals (A) and quantification of mGA (B), fMA (C) and mMA (D) in untreated and FL-926-16 (FL)-treated *db*/*m* control (Ctrl) and *db*/*db* diabetic (Diab) mice (mean ± SD; $n = 5$ per group). Scale bar = 50 μm. *Post hoc* multiple comparison: *$P < 0.05$ versus Ctrl, †$P < 0.05$ versus Diab.

the protective effect exerted by L-carnosine derivatives is due to their ability to scavenge RCS and inhibit AGE formation. As evidence of this, FL-926-16 was not able to reduce *Nlrp3* overexpression induced by CML, the most abundant AGE found *in vivo* (Fu *et al.,* 1996). Moreover, our previous finding that D-carnosine octylester is effective in preventing cytotoxicity induced by HNE, but not by H_2O_2 in cultured mesangial cells, ruled out the possibility that carnosine derivatives provide protection through direct antioxidant effects (Menini *et al.,* 2012).

Taken together, the results from this study support the concept that extensive AGE formation by chronic hyperglycaemia and dyslipidaemia plays a pivotal role in the pathogenesis of diabetic nephropathy, by favouring inflammation and oxidative stress through pathways involving the activation of the NLRP3 inflammasome. In turn, these pathways trigger extracellular matrix remodelling and cell loss through apoptosis, which eventually end up causing a deterioration of renal function. This conclusion is consistent with previous studies indicating that a reduction in oxidative stress (Melhem *et al.,* 2002; DeRubertis *et al.,* 2004) or inflammation (Okada *et al.,* 2003; Tarabra *et al.,* 2009) is effective in preventing or attenuating experimental diabetic glomerulopathy. In addition, our data indicate that a therapeutic strategy aimed at reducing AGE formation and accumulation is effective in attenuating the inflammatory and oxidative pathways triggered by these by-products, thus blunting the onset of diabetes-induced glomerular lesions and stopping the progression of established diabetic nephropathy. As a corollary, treatment with a derivative of the endogenous histidine-containing dipeptide L-carnosine would raise less safety concerns than those associated with the use of pharmacological agents acting on the inflammatory and oxidative stress pathways.

The strengths of this study include the use of a well-established animal model of type 2 diabetes and nephropathy as well as of a novel, rationally designed carnosine derivative with a favourable pharmacokinetic profile, which might be suitable for testing in human subjects. The main limitation is the preliminary nature of these observations, which cannot be readily translated to human diabetic nephropathy.

In conclusion, these data show that treatment with the L-carnosine derivative FL-926-16 provides protection from the development of diabetic glomerulopathy and halts the progression of established diabetic nephropathy. This protection appears to be dependent on a reduced carbonyl stress due to the RCS scavenging activity of FL-926-16, with consequent inhibition of the formation and accumulation of AGEs, which is associated with reduced fibrosis, apoptosis and inflammation, including the activation of the NLRP3

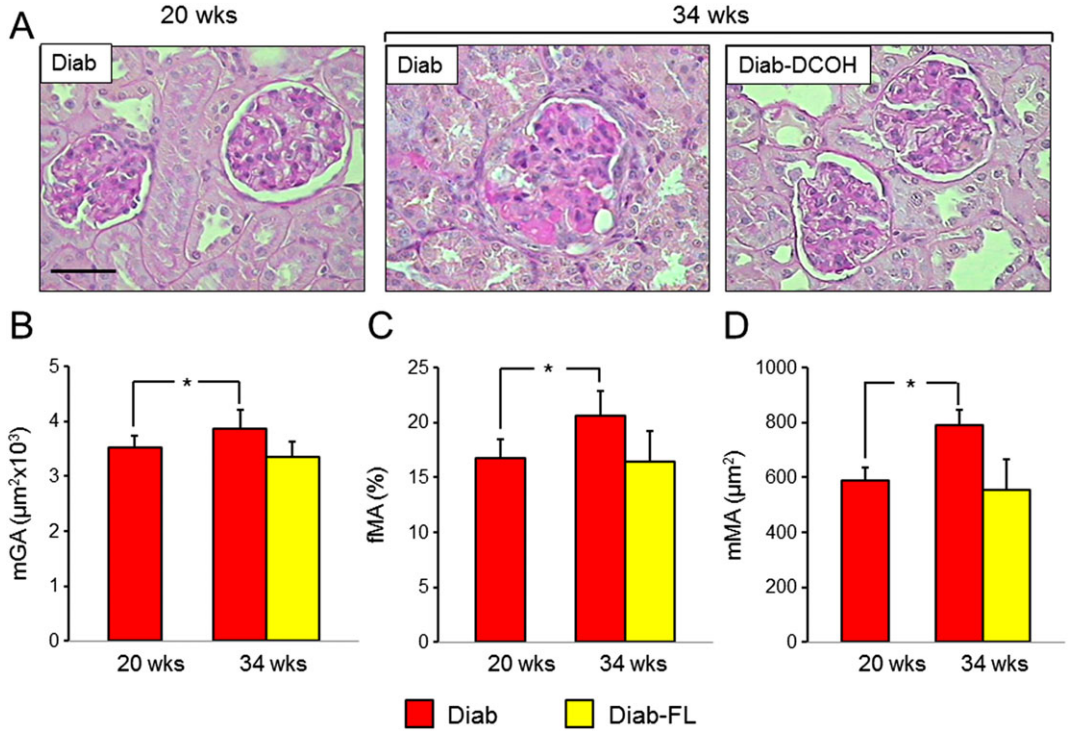

Figure 7

Prevention and regression protocols: renal structure. PAS staining of kidney sections from representative animals (A) and quantification of mGA (B), fMA (C) and mMA (D) in untreated and FL-926-16 (FL)-treated *db*/*db* diabetic mice (Diab and Diab-FL) of 34 weeks of age versus untreated Diab mice of 20 weeks of age (mean ± SD; n = 10 for 20-week-old mice and 5 for 34-week-old mice). Scale bar = 50 μm. Pairwise comparison: *$P < 0.05$ versus Diab-20 weeks.

inflammasome. These results suggest that FL-926-16 might be a suitable strategy for the prevention and treatment of diabetic nephropathy in humans with type 2 diabetes.

Acknowledgements

The Authors thank Cinzia Cataldo for technical assistance in sample collection, coding and histology processing.

This work was supported by a research grant of the Research Foundation of the Italian Society of Diabetology (Associazione Diabete Ricerca ONLUS) to G.P.; Sapienza Università di Roma-Progetti Ateneo 2016 to S.M.; and by an unconditional grant from Flamma S.p.A., Chignolo d'Isola, Italy, that also provided the tested compound FL-926-16 to GP. The sponsors had no role in the design and conduct of the study; collection, management and interpretation of the data; or preparation, review and approval of the manuscript.

Author contributions

C.I. contributed to the conception and design, acquisition of data, analysis and interpretation of data, critical revision of the article for important intellectual content and final approval of the version to be published. C.B.F., C.M.P., A.G., E.S., A.L., M.O. and G.A. contributed to the acquisition of data, critical revision of the article for important intellectual content and final approval of the version to be published. S.M. and G.P. contributed to the conception and design, analysis and interpretation of data, drafting the article and final approval of the version to be published. All Authors agreed to be accountable for all aspects of the work in ensuring that questions related to the accuracy or integrity of any part of the work are appropriately investigated and resolved.

Conflict of interest

G.A. and M.O. are co-authors of the patent application no. WO/2011/080139 on 'Amino alcohol derivatives and their therapeutic activities', which represents the rationale for using FL-926-16 in this work. G.P. is a recipient of an unconditional grant from Flamma S.p.A., Chignolo d'Isola, Italy.

Declaration of transparency and scientific rigour

This Declaration acknowledges that this paper adheres to the principles for transparent reporting and scientific rigour of preclinical research recommended by funding agencies, publishers and other organisations engaged with supporting research.

References

Ahluwalia TS, Lindholm E, Groop LC (2011). Common variants in CNDP1 and CNDP2, and risk of nephropathy in type 2 diabetes. Diabetologia 54: 2295–2302.

Ahmed N (2005). Advanced glycation endproducts – role in pathology of diabetic complications. Diabetes Res Clin Pract 67: 3–21.

Aldini G, Facino RM, Beretta G, Carini M (2005). Carnosine and related dipeptides as quenchers of reactive carbonyl species: from structural studies to therapeutic perspectives. Biofactors 24: 77–87.

Alexander SPH, Kelly E, Marrion NV, Peters JA, Faccenda E, Harding SD *et al*. (2017a). The Concise Guide to PHARMACOLOGY 2017/18: Overview. Br J Pharmacol 174: S1–S16.

Alexander SPH, Fabbro D, Kelly E, Marrion NV, Peters JA, Faccenda E *et al*. (2017b). The Concise Guide to PHARMACOLOGY 2017/18: Catalytic receptors. Br J Pharmacol 174: S225–S271.

Alexander SPH, Fabbro D, Kelly E, Marrion NV, Peters JA, Faccenda E *et al*. (2017c). The Concise Guide to PHARMACOLOGY 2017/18: Enzymes. Br J Pharmacol 174: S272–S359.

Anders HJ, Muruve DA (2011). The inflammasomes in kidney disease. J Am Soc Nephrol 22: 1007–1018.

Bakris GL, Bank AJ, Kass DA, Neutel JM, Preston RA, Oparil S (2004). Advanced glycation end-product cross-link breakers. A novel approach to cardiovascular pathologies related to the aging process. Am J Hypertens 17: 23S–30S.

Block K, Gorin Y, Abboud HE (2009). Subcellular localization of Nox4 and regulation in diabetes. Proc Natl Acad Sci U S A 106: 14385–14390.

Bohlender JM, Franke S, Stein G, Wolf G (2005). Advanced glycation end products and the kidney. Am J Physiol Renal Physiol 289: F645–F659.

Cooper ME (2004). Importance of advanced glycation end products in diabetes-associated cardiovascular and renal disease. Am J Hypertens 17: 31S–38S.

Curtis MJ, Bond RA, Spina D, Ahluwalia A, Alexander SPA, Giembycz MA *et al*. (2015). Experimental design and analysis and their reporting new guidance for publication in BJP. Br J Pharmacol 172: 3461–3471.

Cuzzocrea S, Genovese T, Failla M, Vecchio G, Fruciano M, Mazzon E *et al*. (2007). Protective effect of orally administered carnosine on bleomycin-induced lung injury. Am J Physiol Lung Cell Mol Physiol 292: L1095–L1104.

DeRubertis FR, Craven PA, Melhem MF, Salah EM (2004). Attenuation of renal injury in db/db mice overexpressing superoxide dismutase: evidence for reduced superoxide–nitric oxide interaction. Diabetes 53: 762–768.

Ellis EM (2007). Reactive carbonyls and oxidative stress: potential for therapeutic intervention. Pharmacol Ther 115: 13–24.

Fu MX, Requena JR, Jenkins AJ, Lyons TJ, Baynes JW, Thorpe SR (1996). The advanced glycation end product, Nε-(carboxymethyl) lysine, is a product of both lipid peroxidation and glycoxidation reactions. J Biol Chem 271: 9982–9986.

Gorin Y, Cavaglieri RC, Khazim K, Lee DY, Bruno F, Thakur S *et al*. (2015). Targeting NADPH oxidase with a novel dual Nox1/Nox4 inhibitor attenuates renal pathology in type 1 diabetes. Am J Physiol Renal Physiol 308: F1276–F1287.

Harjutsalo V, Groop PH (2014). Epidemiology and risk factors for diabetic kidney disease. Adv Chronic Kidney Dis 21: 260–266.

Iacobini C, Menini S, Oddi G, Ricci C, Amadio L, Pricci F *et al*. (2004). Galectin-3/AGE-receptor 3 knockout mice show accelerated AGE-induced glomerular injury evidence for a protective role of galectin-3 as an AGE-receptor. FASEB J 18: 1773–1775.

Iacobini C, Menini S, Ricci C, Scipioni A, Sansoni V, Mazzitelli G *et al*. (2009a). Advanced lipoxidation end-products mediate lipid-induced glomerular injury: role of receptor-mediated mechanisms. J Pathol 218: 360–369.

Iacobini C, Menini S, Ricci C, Scipioni A, Sansoni V, Cordone S *et al*. (2009b). Accelerated lipid-induced atherogenesis in galectin-3 deficient mice: role of lipoxidation via receptor-mediated mechanisms. Arterioscler Thromb Vasc Biol 29: 831–836.

Iacobini C, Menini S, Ricci C, Blasetti Fantauzzi C, Scipioni A, Salvi L *et al*. (2011). Galectin-3 ablation protects mice from diet-induced nonalcoholic steatohepatitis. Major scavenging role of galectin-3 in liver. J Hepatol 54: 975–983.

Kilkenny C, Browne W, Cuthill IC, Emerson M, Altman DG (2010). Animal research: reporting *in vivo* experiments: the ARRIVE guidelines. Br J Pharmacol 160: 1577–1579.

Köppel H, Riedl E, Braunagel M, Sauerhoefer S, Ehnert S, Godoy P *et al*. (2011). L-carnosine inhibits high-glucose-mediated matrix accumulation in human mesangial cells by interfering with TGF-β production and signalling. Nephrol Dial Transplant 26: 3852–3858.

Kurata H, Fujii T, Tsutsui H, Katayama T, Ohkita M, Takaoka M *et al*. (2006). Renoprotective effects of l-carnosine on ischemia/reperfusion-induced renal injury in rats. J Pharmacol Exp Ther 319: 640–647.

McGrath JC, Lilley E (2015). Implementing guidelines on reporting research using animals (ARRIVE etc.): new requirements for publication in BJP. Br J Pharmacol 172: 3189–3193.

Melhem MF, Craven PA, Liachenko J, DeRubertis FR (2002). α-Lipoic acid attenuates hyperglycemia and prevents glomerular mesangial matrix expansion in diabetes. J Am Soc Nephrol 13: 108–116.

Menini S, Iacobini C, Ricci C, Oddi G, Pesce C, Pugliese F *et al*. (2007). Ablation of the gene encoding p66Shc protects mice against AGE-induced glomerulopathy by preventing oxidant-dependent tissue injury and further AGE accumulation. Diabetologia 50: 1997–2007.

Menini S, Iacobini C, Ricci C, Scipioni A, Blasetti Fantauzzi C, Giaccari A *et al*. (2012). D-Carnosine octylester attenuates atherosclerosis and renal disease in ApoE null mice fed a Western diet through reduction of carbonyl stress and inflammation. Br J Pharmacol 166: 1344–1356.

Menini S, Iacobini C, Ricci C, Blasetti Fantauzzi C, Pugliese G (2015). Protection from diabetes-induced atherosclerosis and renal disease by D-carnosine-octylester: effects of early vs late inhibition of advanced glycation end-products in Apoe-null mice. Diabetologia 58: 845–853.

Molitch ME, DeFronzo RA, Franz MJ, Keane WF, Mogensen CE, Parving HH *et al*. (2004). Nephropathy in diabetes. Diabetes Care 27 (S1): S79–S83.

Negre-Salvayre A, Coatrieux C, Ingueneau C, Salvayre R (2008). Advanced lipid peroxidation end products in oxidative damage to proteins. Potential role in diseases and therapeutic prospects for the inhibitors. Br J Pharmacol 153: 6–20.

Negrisoli G, Canevotti R, Previtali M, Aldini G, Carini M, Orioli M *et al*. (2011) Amino alcohol derivatives and their therapeutic activities. Patent application No.: WO/2011/080139; International Application No.: PCT/EP2010/070238, Jun 7.

Odetti P, Fogarty J, Sell DR, Monnier VM (1992). Chromatographic quantitation of plasma and erythrocyte pentosidine in diabetic and uremic subjects. Diabetes 41: 153–159.

Okada S, Shikata K, Matsuda M, Ogawa D, Usui H, Kido Y*et al*. (2003). Intercellular adhesion molecule-1-deficient mice are resistant against renal injury after induction of diabetes. Diabetes 52: 2586–2593.

Orioli M, Vistoli G, Regazzoni L, Pedretti A, Lapolla A, Rossoni G *et al*. (2011). Design, synthesis, ADME Properties, and pharmacological activities of β-alanyl-D-histidine (D-Carnosine) prodrugs with improved bioavailability. ChemMedChem 6: 1269–1282.

Peters V, Lanthaler B, Amberger A, Fleming T, Forsberg E, Hecker M *et al*. (2015). Carnosine metabolism in diabetes is altered by reactive metabolites. Amino Acids 47: 2367–2376.

Pugliese G, Pricci F, Leto G, Amadio L, Iacobini C, Romeo G *et al*. (2000). The diabetic milieu modulates the advanced glycation end product-receptor complex in the mesangium by inducing or upregulating galectin-3 expression. Diabetes 49: 1249–1257.

Rajanikant GK, Zemke D, Senut MC, Frenkel MB, Chen AF, Gupta R *et al*. (2007). Carnosine is neuroprotective against permanent focal cerebral ischemia in mice. Stroke 38: 3023–3031.

Reddy VP, Beyaz A (2006). Inhibitors of the Maillard reaction and AGE breakers as therapeutics for multiple diseases. Drug Discov Today 11: 646–654.

Sharma K, McCue P, Dunn SR (2003). Diabetic kidney disease in the db/db mouse. Am J Physiol Renal Physiol 284: F1138–F1144.

Soliman KM, Abdul-Hamid M, Othman AI (2007). Effect of carnosine on gentamicin-induced nephrotoxicity. Med Sci Monit 13: BR73–BR83.

Solini A, Menini S, Rossi C, Ricci C, Santini E, Blasetti Fantauzzi C *et al*. (2013). The purinergic 2X7 receptor participates in renal inflammation and injury induced by high-fat diet: possible role of NLRP3 inflammasome activation. J Pathol 231: 342–353.

Southan C, Sharman JL, Benson HE, Faccenda E, Pawson AJ, Alexander SPH *et al*. (2016). The IUPHAR/BPS guide to PHARMACOLOGY in 2016: towards curated quantitative interactions between 1300 protein targets and 6000 ligands. Nucl Acids Res 44: D1054–D1068.

Tang SC, Arumugam TV, Cutler RG, Jo DG, Magnus T, Chan SL *et al*. (2007). Neuroprotective actions of a histidine analogue in models of ischemic stroke. J Neurochem 101: 729–736.

Tarabra E, Giunti S, Barutta F, Salvidio G, Burt D, Deferrari G *et al*. (2009). Effect of the monocyte chemoattractant protein-1/CC chemokine receptor 2 system on nephrin expression in streptozotocin-treated mice and human cultured podocytes. Diabetes 58: 2109–2118.

Tuttle KR, Bakris GL, Bilous RW, Chiang JL, de Boer IH, Goldstein-Fuchs J *et al*. (2014). Diabetic kidney disease: a report from an ADA Consensus Conference. Am J Kidney Dis 64: 510–533.

Vistoli G, Orioli M, Pedretti A, Regazzoni L, Canevotti R, Negrisoli G *et al*. (2009). Design, synthesis, and evaluation of carnosine derivatives as selective and efficient sequestering agents of cytotoxic reactive carbonyl species. Chem Med Chem 4: 967–975.

Wendt T, Tanji N, Guo J, Hudson BI, Bierhaus A, Ramasamy R *et al*. (2003). Glucose, glycation, and RAGE: implications for amplification of cellular dysfunction in diabetic nephropathy. J Am Soc Nephrol 14: 1383–1395.

Supporting Information

Additional Supporting Information may be found online in the supporting information tab for this article.

https://doi.org/10.1111/bph.14070

Figure S1 Prevention protocol: western blot analysis for collagen IV and F4/80. Western blot analysis for collagen IV a1 chain (*Panel A*) and F4/80 (*Panel B*) protein levels in representative animals and relative band densitometry analysis in untreated and FL-926-16 (FL)-treated *db*/*m* control (Ctrl) and *db*/*db* diabetic (Diab) mice (mean ± SD; $n = 5$ per group). The Y axis label "Relative level" indicates fold of mean value of Ctr (db/m control) mice. *Post hoc* multiple comparison: *$P < 0.05$ *vs* Ctrl, †$P < 0.05$ *vs* Diab.
Table S1 Assays used for qRT-PCR analysis.